Experimental Observation of Dynamical Localization in Laser-Kicked Molecular Rotors

M. Bitter and V. Milner
Department of Physics & Astronomy and The Laboratory for Advanced Spectroscopy and Imaging Research (LASIR), The University of British Columbia, V6T 1Z1 Vancouver, Canada

(Received 17 April 2016; revised manuscript received 18 August 2016; published 29 September 2016)

The periodically kicked rotor is a paradigm system for studying quantum effects on classically chaotic dynamics. The wave function of the quantum rotor localizes in angular momentum space, similarly to Anderson localization of the electronic wave function in disordered solids. Here, we observe dynamical localization in a system of true quantum rotors by subjecting nitrogen molecules to periodic sequences of femtosecond pulses. Exponential distribution of the molecular angular momentum—the hallmark of dynamical localization—is measured directly by means of coherent Raman scattering. We demonstrate the suppressed rotational energy growth with the number of laser kicks and study the dependence of the localization length on the kick strength. Because of its quantum coherent nature, both timing and amplitude noise are shown to destroy the localization and revive the diffusive growth of energy.

DOI: 10.1103/PhysRevLett.117.144104

The periodically kicked rotor is one of the simplest systems whose classical motion may become chaotic, leading to an unbounded diffusive growth of its energy with the number of kicks. In contrast, the energy growth of a quantum kicked rotor (QKR) is suppressed due to the interference of quantum interaction pathways [1,2]. This effect of dynamical localization has been linked to Anderson localization in solids [3]. Much like a quantum particle localizes in the real space of a disordered one-dimensional lattice, the QKR localizes in the "lattice" of its rotational states [4]. The wave function of the quantum rotor does not grow wider with every consecutive kick, but instead localizes near the initial rotational state, with the probability amplitude falling exponentially away from it.

Dynamical localization has been studied experimentally in Rydberg atoms [5–8] and a cold-atom analogue of the QKR [9–14], yet it has never been observed in the system of true quantum rotors. A natural choice for a system of quantum rotors—a diatomic molecule subject to short kicks from a pulsed external field (microwave, optical, or THz), has been discussed in multiple theoretical proposals [15–18]. In a series of recent works [17,19–21], Averbukh and co-workers suggested a strategy to observe and study a number of QKR effects in an ensemble of molecules exposed to a periodic sequence of ultrashort laser pulses. The effects of a quantum resonance [22,23] and Bloch oscillations [24] have been verified experimentally. An onset of dynamical localization in laser-induced molecular alignment has been reported [25], but its two distinct signatures and necessary components—the exponential distribution of the localized wave function and the suppressed growth of the rotational energy—have not been shown.

The difficulty of demonstrating dynamical localization with molecular rotors stems from a number of experimental challenges. First, the need to assess the shape of the rotational distribution calls for a sensitive detection method capable of resolving individual rotational states over a range of 2 orders of magnitude [19]. Second, for the localized state not to be smeared out due to the averaging over the initial thermal distribution, the latter must be narrowed down to as close to a single rotational state as possible, requiring cold molecular samples. Finally, an important test of dynamical localization, the recovery of classical diffusion under the influence of noise and decoherence, demonstrated experimentally with atoms [7,10,26–28] and theoretically with molecular QKR [19], requires long sequences of more than 20 strong kicks.

In this Letter, we address all three of the above challenges and study the rotational dynamics of nitrogen molecules, cooled down to 27 K in a supersonic expansion and kicked by a periodic series of 24 laser pulses. We use state-resolved coherent Raman spectroscopy to demonstrate the exponential shape of the created rotational wave packet, indicative of dynamical localization. The dependence of the rotational distribution on the number of pulses and their strength is investigated. Our ability to resolve individual rotational states allows for a direct extraction of the absorbed energy, whose growth is shown to cease completely after as few as three pulses. To confirm the coherent nature of the observed localization, we study the effect of both timing noise and amplitude noise, which are shown to yield a nonexponential distribution of angular momenta and revive the diffusive growth of energy. Our results are in good agreement with the theoretical analysis of Floß, Fishman, and Averbukh [19] and our own numerical simulations.

We developed an optical setup capable of generating high-intensity trains of femtosecond pulses [29]. Exposing nitrogen molecules to these pulses results in coherent

rotation, which modulates the refractive index of the gas. Consequently, the spectrum of a weak probe light acquires Raman sidebands shifted with respect to its central frequency and polarized orthogonally to its initial polarization [30,31]. By passing the probe pulses through an analyzer set at 90° with respect to the input probe polarization, we detect the rotational Raman spectrum of kicked molecules with a dynamic range of 4 orders of magnitude in intensity. The details of the experimental setup are given in the Supplemental Material [32].

Consider a coherent superposition of two rotational states, $\psi_{J,M}(t) = c_{J,M}e^{-2\pi i E_J t/h}|J, M\rangle + c_{J+2,M}e^{-2\pi i E_{J+2} t/h}|J+2, M\rangle$, created by a linearly polarized pump field. Here, J and M are the molecular angular momentum and its projection on the vector of pump polarization, $E_J = hcBJ(J+1)$ is the rotational energy of a rigid rotor with the rotational constant B, c is the speed of light in vacuum, and h is the Planck's constant. The coherent dynamics of such a wave packet will result in a Raman peak with a J-dependent frequency shift $\Delta\omega_J = (E_{J+2} - E_J)/h = 2Bc(2J+3)$. Owing to the selection rules for a two-photon excitation process, $\Delta J = 0, \pm 2$ and $\Delta M = 0$, the superposition $\psi_{J,M}(t)$ can originate from any initially populated thermal state $|J' = J \pm 2k, M' = M\rangle$, where k is an integer. Hence, the intensity of the observed Raman peak will be proportional to the modulus squared of the induced coherence, $I_J \propto \sum_M \langle |c^*_{J,M} c_{J+2,M}|^2 \rangle_{J',M'}$, summed over the degenerate M sublevels and averaged over the initial thermal mixture.

Note that if the initial ensemble contained only one populated level $|J' = J_0, M' = M_0\rangle$, the strength of the Raman signal would reduce to $I_J \propto P_{J,M_0} P_{J+2,M_0}$, where $P_{J,M} = |c_{J,M}|^2$ is the rotational population. For localized and nonlocalized dynamics of the QKR, we expect exponential or Gaussian population distributions, respectively [26,35]. In either case, the Raman spectrum can be further simplified to $I_J \propto (P_{J,M_0})^2$, offering the direct measure of the rotational population. As we show below, this proportionality holds even at a nonzero temperature of molecules in our supersonic jet, when the Raman signal is produced by a number of independent rotational wave packets originating from different initial states $|J', M'\rangle$. At 27 K most of the population is initially at $J' = 2$ [36]. Thus, the smallness of $M' = 0, \pm 1, \pm 2$ with respect to the angular momentum of the majority of states in the final wave packet results in an interaction Hamiltonian which to a good degree of approximation does not depend on M' [37]. Having all molecules in the thermal ensemble respond to the laser field in an almost identical way enables us to extract rotational populations from the Raman signal as $P_J = a\sqrt{I_J}$, with the coefficient a found from normalizing the total population to unity.

To determine the exact pulse intensity in the interaction region, we tune the period of the pulse train to the rotational period of a wave packet consisting of two rotational states with $J = 2$ and $J = 4$ [38]. Fitting the frequency of the ensuing Rabi oscillations between the two states provides an accurate way of measuring the intensity of the pump pulses [39]. It is often expressed in the dimensionless units of "kick strength" $P = \Delta\alpha/(4\hbar)\int \mathcal{E}^2(t)dt$, where $\Delta\alpha$ is the polarizability anisotropy of the molecule and $\mathcal{E}$ the temporal envelope of the pulse. The kick strength reflects the typical amount of angular momentum (in units of $\hbar$) transferred from the laser pulse to the molecule [34]. By amplifying a sequence of 24 pulses in a multi-pass amplifier, we were able to reach kick strengths of up to $P = 3$ per pulse (2×10^{13} W/cm^2).

Figure 1(a) shows a set of 20 Raman spectra, obtained with 20 different *periodic* pulse trains. Localized states in the quantum kicked rotor are known to exist away from the quantum resonances, i.e., when the time between kicks is not equal to a rational fraction of the revival period $T_{\rm rev} = (2Bc)^{-1}$ [4]. To avoid strong fractional resonances of low orders, we chose 10 evenly spaced pulse train periods T in each of the two intervals, $10/13 < T/T_{\rm rev} < 5/6$ and $7/8 < T/T_{\rm rev} < 13/14$, with $T_{\rm rev} = 8.38$ ps for molecular nitrogen $^{14}N_2$. The Raman frequency shift (horizontal axis) has been converted to the rotational quantum number J.

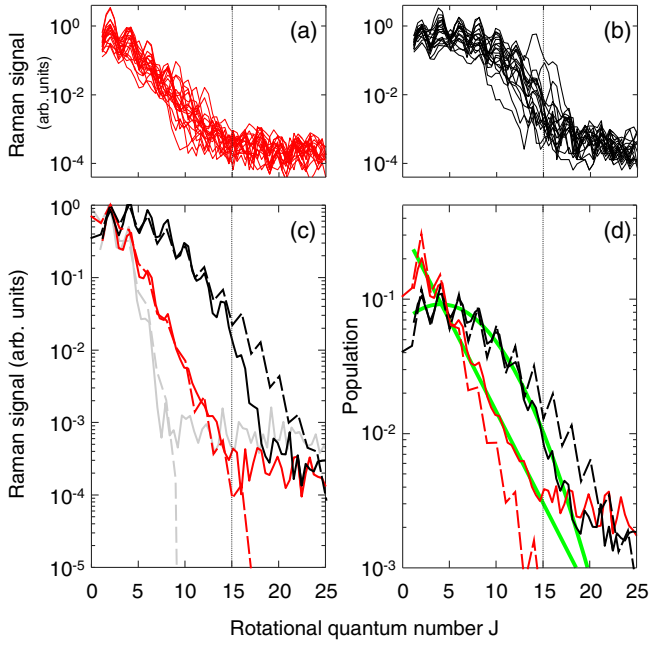

FIG. 1. Rotational Raman spectrum of nitrogen molecules excited with a train of $N = 24$ pulses at a kick strength of $P = 2.3$ for 20 different periodic (a) and nonperiodic (b) sequences. (c) The average experimental distributions (solid lines) are compared to the numerical simulations (dashed lines) for both the periodic (middle red lines) and the nonperiodic (upper black lines) pulse trains. The initial distribution is shown by the lower gray lines. (d) The exact calculated populations (dashed lines) and the approximate populations (solid lines), retrieved from the experimental Raman signal as discussed in the text. The retrieved populations are fitted with an exponential or Gaussian function (thick green lines). The dotted vertical line represents the excitation limit due to the finite pulse duration.

The average Raman signal is plotted with the solid red line in Fig. 1(c). It decays exponentially across 4 orders of magnitude and 15 rotational states, and can be clearly distinguished from the initial Boltzmann distribution (solid gray line). The remaining oscillations are a consequence of the nuclear spin statistics of nitrogen, which dictates the 2:1 ratio for the two independent rotational progressions consisting of only even and only odd values of angular momentum. The exact shape of each individual distribution in Fig. 1(a) depends on the period of the corresponding train and is affected by its proximity to fractional quantum resonances of higher orders. In Fig. 1(d), the solid red line illustrates the distribution of the rotational population, extracted from the average Raman signal according to $P_J \propto \sqrt{I_J}$. The evident exponential shape, highlighted by an exponential fit (thick green line) with a localization length ($1/e$ width) $J_{\mathrm{loc}} = 3.2$, is a hallmark of dynamical localization in this true QKR system.

To confirm the coherent nature of the observed localization, we check the effect of "timing noise" by repeating the same measurement with a set of 20 *nonperiodic* pulse trains. The kick strength is set to the same value of $P = 2.3$ per pulse, but the time intervals between the 24 pulses in each train are randomly varied (using the pulse shaping technique, described in Supplemental Material [32]) around the mean value of 0.85 T_{rev} with a standard deviation of 33%. All the individual Raman spectra, their average, and the population distribution retrieved from it [solid black lines in Figs. 1(b), 1(c), and 1(d), respectively] show a qualitatively different nonexponential shape. As expected for a quantum kicked rotor, dynamical localization is destroyed by noise, while classical diffusion, with its characteristic Gaussian distribution of angular momentum (thick green line, $1/e$ width of $J_{\mathrm{diff}} = 7.4$), is recovered.

In Figs. 1(c) and 1(d), we also compare our experimental data to the results of numerical simulations, shown with dashed lines. The latter are carried out by solving the Schrödinger equation for nitrogen molecules interacting with a sequence of δ kicks [32]. We calculate the complex amplitudes $c_{J,M}$ of all rotational states in the wave packet created from each initially populated state $|J', M'\rangle$. Averaging over the initial thermal mixture, we simulate the expected Raman signals $I_J \propto \sum_M \langle |c^*_{J,M} c_{J+2,M}|^2 \rangle_{J',M'}$, and find the exact populations $P_J = \sum_M \langle |c_{J,M}|^2 \rangle_{J',M'}$.

In the case of a periodic sequence of kicks, the observed Raman line shape [Fig. 1(c)] is in good agreement with the numerical result down to the instrumental noise floor around $I_J \approx 10^{-4}$. Calculated populations [Fig. 1(d)] demonstrate the anticipated exponential decay with the rotational quantum number, but deviate slightly from the experimentally retrieved distribution. We attribute this discrepancy to the small finite thermal width of the initial rotational distribution, not accounted for in approximating the populations by $\sqrt{I_J}$, as discussed earlier.

When the timing noise is simulated numerically, both the calculated Raman response and the population distributions show a nonexponential shape and match the experimental observations below $J \approx 15$. The disagreement at higher values of angular momentum is because of the finite duration of our laser pulses (130 fs full width at half maximum), which is not taken into account in the simulations. At $J \geq 15$ (i.e., to the right of the dotted vertical line), a nitrogen molecule rotates by $\gtrsim 90°$ during the length of the pulse, which lowers its effective kick strength and suppresses further rotational excitation.

Figure 2 shows the evolution of the rotational distribution with the number of kicks N. For the case of a periodic pulse train illustrated in Fig. 2(a), the distribution becomes exponential within a few kicks and hardly changes after that: $J_{\mathrm{loc}} = 3.1$, 3.3, and 3.3 for $N = 8$, 16, and 24, respectively. In sharp contrast, the line shape in Fig. 2(b) for nonperiodic kicking remains Gaussian and keeps broadening with increasing N: $J_{\mathrm{diff}} = 5.6$, 6.2, and 7.9. This behavior demonstrates the destruction of dynamical localization by timing noise and clearly distinguishes it from other mechanisms of suppressed rotational excitation.

The dependence of the rotational distribution on the strength of periodic and nonperiodic kicks is shown in Fig. 3(a) and 3(b), respectively. As expected for a periodically kicked quantum rotor, the localization length grows with increasing P: $J_{\mathrm{loc}} = 2.2$, 2.9, and 4.7 for $P = 1$, 2, and 3, respectively. The line shape remains exponential below the cutoff value of $J \approx 15$ discussed earlier. For each kick strength, the Gaussian distribution after a noisy pulse sequence is significantly broader ($J_{\mathrm{diff}} = 6.7$, 7.5, and 10.8) and lies well above its localized counterpart, despite being equally affected by the cutoff, thus confirming the universality of the observed dynamics.

Owing to our state-resolved detection, the total rotational energy of a molecule can be calculated as $\sum_J E_J P_J$, with populations P_J extracted from the observed Raman spectra I_J. The rotational energy is plotted as a function of the number of kicks for multiple excitation scenarios in Fig. 4. For periodic kicking, the retrieved energy (red squares) increases during the first three kicks, after which its further growth is completely suppressed—a prominent feature of dynamical localization in the QKR. Breaking the periodicity of the pulse sequence with timing noise results in the recovery of the classical diffusion, manifested by the continuously increasing rotational energy of the rotors (black circles). The sublinear growth rate is due to the finite duration of our laser pulses, mentioned earlier. As expected, dynamical localization is also susceptible to "amplitude noise." When the amplitudes of a periodic pulse sequence randomly vary with a standard deviation of 41% (introduced by the pulse shaper), the steady energy growth is again revived (blue triangles). The numerically calculated rotational energies for the three cases of a periodic, a nonperiodic and a noisy-amplitude pulse train

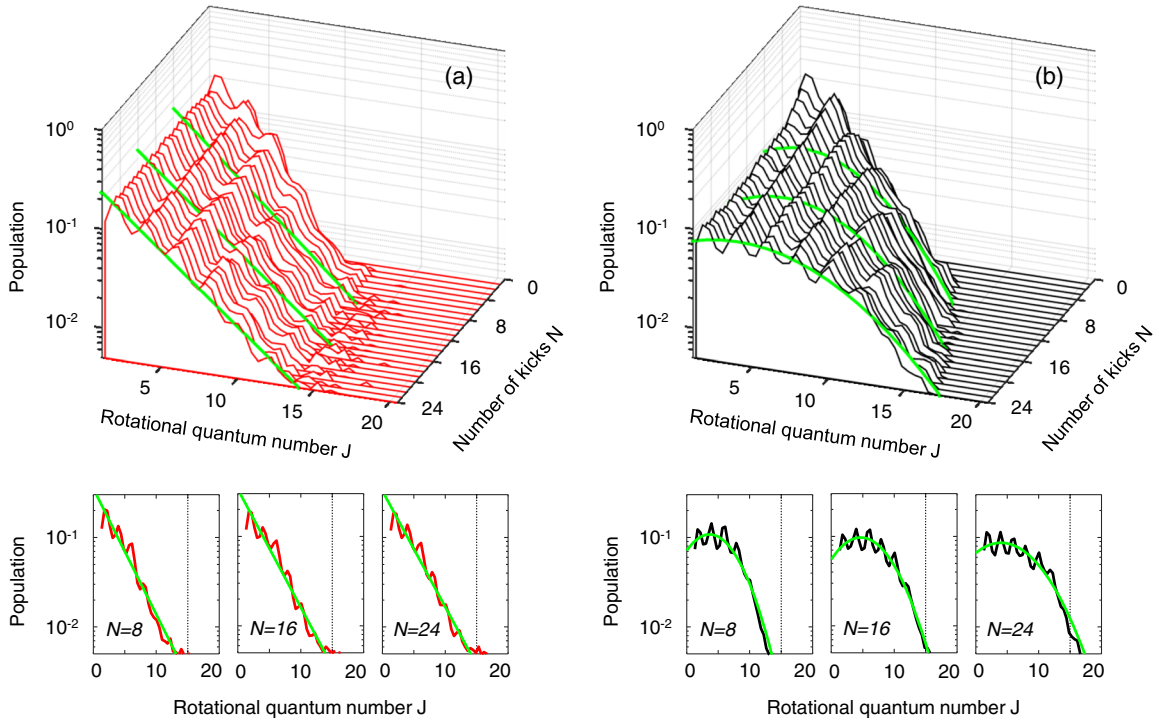

FIG. 2. Evolution of the molecular angular momentum distribution with the number of kicks N (each of strength $P = 2.3$) for a periodic (a) and nonperiodic (b) excitation. Respective exponential and Gaussian fits, shown individually in the lower plots, indicate the changes of the distributions at $N = 8$, 16, and 24 (thick green lines, see text for distribution widths). The dotted vertical line represents the excitation limit due to the finite pulse duration.

are shown with the dashed red, dotted black, and dash-dotted blue lines, respectively. Owing to the approximation in retrieving the rotational populations from Raman spectra, the calculations are expected to overestimate the true rotational energies (except when the finite pulse duration becomes important). Yet, they qualitatively agree with the theoretical predictions.

In summary, we have demonstrated experimentally the effect of dynamical localization in a system of true quantum kicked rotors—a gas of nitrogen molecules exposed to a periodic sequence of intense laser pulses. Cold initial conditions and a high-sensitivity state-resolved detection enabled us to observe the distribution of the molecular angular momenta evolving into an exponential line shape, characteristic of a localized state. The suppressed growth of rotational energy, and the noise-induced recovery of the classical diffusion have also been presented. Our work complements previous studies of the QKR in a system of

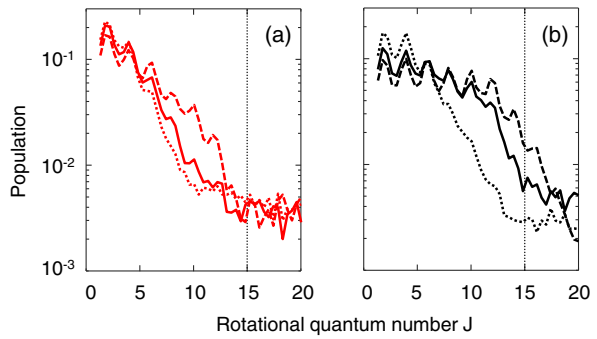

FIG. 3. Angular momentum distributions after 24 pulses of a periodic (a) and nonperiodic (b) train for three kick strengths: $P = 1$ (dotted line), $P = 2$ (solid line), and $P = 3$ (dashed line). The dotted vertical line represents the excitation limit due to the finite pulse duration.

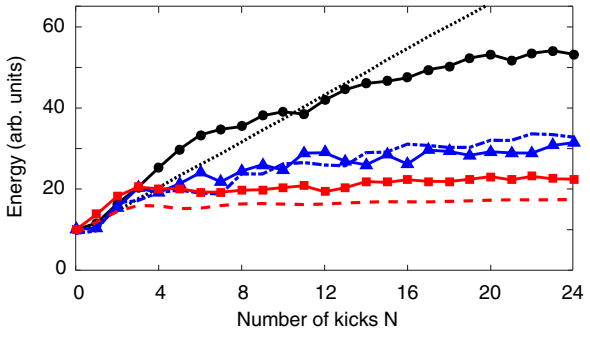

FIG. 4. Rotational energy as a function of the number of kicks N with a mean strength of $P = 2.3$. Compared are the experimentally retrieved energies (connected symbols) with the numerically calculated ones (lines), for a periodic sequence (red squares, dashed line), and the same sequence after the introduction of amplitude noise (blue triangles, dash-dotted line) or timing noise (black circles, dotted line).

cold atoms. In contrast to the latter, true molecular rotors exhibit discrete energy spectra and offer opportunities for investigating new quantum phenomena such as edge localization [21] or the effects of the centrifugal distortion and rotational decoherence on QKR dynamics [20]. Exploring the possibility of quantum coherent control in these classically chaotic molecular systems is of great interest [40].

The authors would like to thank J. Floß and I. Sh. Averbukh for stimulating discussions and J. Floß for his help with numerical calculations. This research has been supported by the grants from CFI, BCKDF and NSERC.

[1] G. Casati, B. Chirikov, F. Izraelev, and J. Ford, in *Stochastic Behavior in Classical and Quantum Hamiltonian Systems*, Lecture Notes in Physics Vol. 93, edited by G. Casati and J. Ford (Springer, Berlin, 1979), pp. 334–352.
[2] F. M. Izrailev and D. L. Shepelyanskii, Theor. Math. Phys. **43**, 553 (1980).
[3] P. W. Anderson, Phys. Rev. **109**, 1492 (1958).
[4] S. Fishman, D. R. Grempel, and R. E. Prange, Phys. Rev. Lett. **49**, 509 (1982).
[5] E. J. Galvez, B. E. Sauer, L. Moorman, P. M. Koch, and D. Richards, Phys. Rev. Lett. **61**, 2011 (1988).
[6] J. E. Bayfield, G. Casati, I. Guarneri, and D. W. Sokol, Phys. Rev. Lett. **63**, 364 (1989).
[7] R. Blümel, A. Buchleitner, R. Graham, L. Sirko, U. Smilansky, and H. Walther, Phys. Rev. A **44**, 4521 (1991).
[8] M. T. Frey, F. B. Dunning, C. O. Reinhold, S. Yoshida, and J. Burgdörfer, Phys. Rev. A **59**, 1434 (1999).
[9] F. L. Moore, J. C. Robinson, C. F. Bharucha, B. Sundaram, and M. G. Raizen, Phys. Rev. Lett. **75**, 4598 (1995).
[10] H. Ammann, R. Gray, I. Shvarchuck, and N. Christensen, Phys. Rev. Lett. **80**, 4111 (1998).
[11] M. B. d'Arcy, R. M. Godun, M. K. Oberthaler, D. Cassettari, and G. S. Summy, Phys. Rev. Lett. **87**, 074102 (2001).
[12] M. Sadgrove, S. Wimberger, S. Parkins, and R. Leonhardt, Phys. Rev. Lett. **94**, 174103 (2005).
[13] C. Ryu, M. F. Andersen, A. Vaziri, M. B. d'Arcy, J. M. Grossman, K. Helmerson, and W. D. Phillips, Phys. Rev. Lett. **96**, 160403 (2006).
[14] J. Chabé, G. Lemarié, B. Grémaud, D. Delande, P. Szriftgiser, and J. C. Garreau, Phys. Rev. Lett. **101**, 255702 (2008).
[15] R. Bluemel, S. Fishman, and U. Smilansky, J. Chem. Phys. **84**, 2604 (1986).
[16] J. Gong and P. Brumer, J. Chem. Phys. **115**, 3590 (2001).
[17] J. Floß and I. Sh. Averbukh, Phys. Rev. A **86**, 021401 (2012).
[18] L. Matsuoka, Phys. Rev. A **91**, 043420 (2015).
[19] J. Floß, S. Fishman, and I. Sh. Averbukh, Phys. Rev. A **88**, 023426 (2013).
[20] J. Floß and I. Sh. Averbukh, Phys. Rev. Lett. **113**, 043002 (2014).
[21] J. Floß and I. Sh. Averbukh, Phys. Rev. E **91**, 052911 (2015).
[22] J. P. Cryan, P. H. Bucksbaum, and R. N. Coffee, Phys. Rev. A **80**, 063412 (2009).
[23] S. Zhdanovich, C. Bloomquist, J. Floß, I. Sh. Averbukh, J. W. Hepburn, and V. Milner, Phys. Rev. Lett. **109**, 043003 (2012).
[24] J. Floß, A. Kamalov, I. Sh. Averbukh, and P. H. Bucksbaum, Phys. Rev. Lett. **115**, 203002 (2015).
[25] A. Kamalov, D. W. Broege, and P. H. Bucksbaum, Phys. Rev. A **92**, 013409 (2015).
[26] B. G. Klappauf, W. H. Oskay, D. A. Steck, and M. G. Raizen, Phys. Rev. Lett. **81**, 1203 (1998).
[27] V. Milner, D. A. Steck, W. H. Oskay, and M. G. Raizen, Phys. Rev. E **61**, 7223 (2000).
[28] W. H. Oskay, D. A. Steck, and M. G. Raizen, Chaos, Solitons Fractals **16**, 409 (2003).
[29] M. Bitter and V. Milner, Appl. Opt. **55**, 830 (2016).
[30] O. Korech, U. Steinitz, R. J. Gordon, I. Sh. Averbukh, and Y. Prior, Nat. Photonics **7**, 711 (2013).
[31] A. Korobenko, A. A. Milner, and V. Milner, Phys. Rev. Lett. **112**, 113004 (2014).
[32] See Supplemental Material at http://link.aps.org/supplemental/10.1103/PhysRevLett.117.144104, which includes Refs. [33,34], for details on the optical setup and the numerical simulation.
[33] A. M. Weiner, Rev. Sci. Instrum. **71**, 1929 (2000).
[34] S. Fleischer, Y. Khodorkovsky, Y. Prior, and I. Sh. Averbukh, New J. Phys. **11**, 105039 (2009).
[35] D. Cohen, Phys. Rev. A **44**, 2292 (1991).
[36] The rotational temperature in the experiment was retrieved numerically by fitting the initial distribution obtained after a single weak pulse, plotted in Fig. 1(c).
[37] We have verified this approximation numerically.
[38] M. Bitter and V. Milner, Phys. Rev. A **93**, 013420 (2016).
[39] The details of this method will be discussed in a future publication.
[40] J. Gong and P. Brumer, Annu. Rev. Phys. Chem. **56**, 1 (2005).